The fate of the α-vacuum

Hael Collins,* R. Holman,† and Matthew R. Martin‡
Department of Physics, Carnegie Mellon University, Pittsburgh, Pennsylvania 15213, USA
(Received 10 June 2003; published 19 December 2003)

de Sitter space-time has a one complex parameter family of invariant vacua for the theory of a free, massive scalar field. For most of these vacua, in an interacting scalar theory the one loop corrections diverge linearly for large values of the loop momentum. These divergences are not of a form that can be removed by a de Sitter invariant counterterm, except in the case of the Euclidean, or Bunch-Davies, vacuum.

DOI: 10.1103/PhysRevD.68.124012 PACS number(s): 04.62.+v, 11.10.Gh, 98.80.Cq, 98.80.Qc

I. INTRODUCTION

The importance of understanding quantum field theory in de Sitter space, the space-time associated with a positive cosmological constant, has been heightened by recent observations of both the early and late Universe. The dramatic results of Wilkinson Microwave Anisotropy Probe [1] have provided further strong evidence that the universe underwent a rapid inflationary expansion. Both the large-angle anticorrelation in the temperature-polarization cross-power spectrum and the nearly flat spectral index are consistent with the predictions of inflation. More surprisingly, the dimming of the type Ia supernovae seen by the Supernova Search Team [2] and the Supernova Cosmology Project [3], combined with other observations, is yielding a new standard picture for the contents of the universe, the largest component of which is a dark energy whose properties are consistent with a positive cosmological constant.

A striking difference between de Sitter and flat space-time is the richer vacuum structure of the former. For a free scalar field in a Minkowski space, there exists an essentially unique Poincaré invariant vacuum state. In contrast, for a de Sitter background, Mottola [4] and Allen [5] discovered an infinite family of vacua for the quantum theory of a free massive scalar field that are invariant under the isometries of de Sitter space. These vacua can be parametrized by a single complex number, α, and are usually called the α-vacua. Most of these α-vacua have a host of peculiar features, such as a mixture of positive and negative frequency modes at short distances and a nonthermal behavior that violates the principle of detailed balance. Only one of these states, the Euclidean or Bunch-Davies [6] vacuum, behaves thermally when viewed by an Unruh detector [7] and reduces to the Minkowski vacuum as we take the cosmological constant to zero. The preferred role of the Euclidean vacuum was also shown by [8]. The assumption that the universe was at least approximately in the Euclidean vacuum underlies the successful predictions of inflation for the calculation of the density fluctuations which produced the temperature anisotropies in the cosmic microwave background radiation.

Despite their unappealing features, the α-vacua are perfectly valid vacua for a free scalar field. If they cannot be shown to be unphysical, then their existence would undercut some of the robustness of the inflationary paradigm—we would need to explain how the epoch prior to inflation managed to place the universe in the Euclidean vacuum rather than one of the other infinite family of α-vacua. For example, the regularization needed by the energy-momentum tensor even for the free theory in the α-vacuum is not generally compatible with that needed after inflation [9].

A complication in formulating quantum field theory in de Sitter space is its lack of a well-defined *S*-matrix. In an interacting theory we have two sources of time dependence for matrix elements—one induced by any inherent time dependence of the background geometry and another introduced by the interactions. In such a system, it is therefore appropriate only to ask time dependent questions—to study how a matrix element evolves from a given initial state.

Schwinger [10] and Keldysh [11] developed a formalism to solve for this finite time evolution. In their approach, we specify the state of the system at an initial time and then evolve to a finite time later. Here, both the ''in'' and ''out'' states correspond to the same state and are evolved together when we evaluate the expectation value of an operator—in effect this formalism evaluates matrix elements between two ''in'' states. The Schwinger-Keldysh formalism is thus ideally suited for studying the behavior of the α-vacua in the presence of interactions. We place the system initially in an α-vacuum and then study whether a sensible evolution results. Since the quantum field theory only is evolved over a finite interval, our results are relevant not only for the more formal question of the α-vacua in an eternal de Sitter background but also for the phenomenological problem of a finite epoch of inflation.

The methods established here can also be applied to any initial state, such as the ''truncated α-vacua'' of [12]. In these vacua, the short-distance behavior of the α-vacua is modified either in accord with some specific theory, such as the stringy uncertainty relation of [13,14], or simply by truncating the α-mode functions above some energy scale to reflect our ignorance of the new physics [12,15–18]. We here address the formal case of a pure α-vacuum and shall study the truncated case later in [19].

In this article, we show that an interacting scalar field theory in a general α-vacua contains linear divergences which cannot be removed with a de Sitter invariant renor-

*Electronic address: hael@cmuhep2.phys.cmu.edu
†Electronic address: rh4a@andrew.cmu.edu
‡Electronic address: mmartin@cmu.edu

malization prescription. These divergences appear in the one loop corrections and are present for arbitrarily weak interactions. The specific example we study is the expectation value of the number of Euclidean particles in an α-vacuum. The divergences appear in the high momentum region of the loop integral. We show that they only vanish for the Euclidean vacuum, which is completely renormalizable.

The subject of the α-vacua for an interacting theory has also been recently investigated in related work [20,21]. Both of these works essentially studied the corrections to the two-point correlation function obtained between an "in" α-state and an "out" state given by the α-state at a later time. Banks and Mannelli [20] found that the interacting theory in the α-vacuum required nonlocal counterterms while Einhorn and Larsen [21] found pinched singularities in the loop corrections. These features provided highly suggestive evidence that the α-vacua are pathological in the presence of interactions. Some attempts to modify the theory to avoid these problems appear in [22,23].

We begin with a review of the de Sitter invariant vacua for a free scalar field in Sec. II. This section also shows the form of the Wightman functions in conformally flat coordinates. Section III derives the expectation value of an operator in an interacting theory based on the Schwinger-Keldysh formalism. In Sec. IV we calculate the change in the number of Euclidean particles in an α-vacuum due to a cubic interaction and show that in the presence of this interaction, the expectation value is renormalizable for the Euclidean vacuum while an unrenormalizable divergence appears for the α-vacuum. Section V explores the origin of these divergences in the α-vacua in a more general setting. We derive the necessary conditions for these divergences to arise and show how they can appear in a general interacting scalar field theory. Section VI summarizes our results and suggests future applications for this formalism.

II. GREEN'S FUNCTIONS

In this section we review the rich vacuum structure of a free scalar field in de Sitter space [24]. We derive the form of the Wightman function and eventually the Feynman propagator in conformally flat coordinates. These Green's functions will be used later for studying the interacting theory.

The most straightforward method for demonstrating the existence of a family of de Sitter invariant vacua is to evaluate the two-point Wightman function for a free massive scalar field in an α-vacuum. For this purpose it is useful to use a coordinate system that covers the entire space-time. Such coordinates are not, however, those best suited for more explicit calculations. Therefore, throughout this article we shall study de Sitter space using conformally flat coordinates,

$$ds^2=\frac{d\eta^2-d\vec{x}^2}{H^2\eta^2}, \tag{2.1}$$

with $\eta\in[-\infty,0]$ which cover half of de Sitter space [25]. The other half of the space is covered by a set of coordinates with $\eta\to-\eta$. These coordinates are simply related to the standard coordinates used in inflation,

$$ds^2=dt^2-e^{2Ht}\,d\vec{x}^2, \tag{2.2}$$

through $\eta=-H^{-1}e^{-Ht}$. H is the Hubble constant and is related to the cosmological constant by $\Lambda=6H^2$.

A. The Euclidean vacuum

To an observer capable only of probing length scales on which the curvature of de Sitter space is not apparent, the space-time appears approximately flat. For the high energy modes then, this observer can apply the same prescription for defining positive and negative frequency modes as in Minkowski space. The vacuum state annihilated by the operators $a_{\vec{k}}^E$ associated with these modes corresponds to the Euclidean vacuum.

The Euclidean vacuum possesses many desirable properties in addition to matching with the Minkowski vacuum at short distances or as $H\to 0$. It corresponds to the unique state whose Wightman function is analytic when continued to the lower half of the Euclidean sphere. Moreover, an Unruh detector placed in the Euclidean vacuum satisfies the principle of detailed balance as though it were immersed in a thermal system at the de Sitter temperature, $T_{\rm dS}=H/2\pi$ [24].

If we denote the Euclidean vacuum by $|E\rangle$, the Euclidean Wightman function for a free massive scalar field $\Phi(x)$ is defined by

$$G_E(x,x')\equiv\langle E|\Phi(x)\Phi(x')|E\rangle. \tag{2.3}$$

Since the metric is spatially flat, the expansion of the scalar field $\Phi(x)$ in creation and annihilation operators $a_{\vec{k}}^{E\dagger}, a_{\vec{k}}^E$ for the vacuum state $|E\rangle$ is

$$\Phi(\eta,\vec{x})=\int\frac{d^3\vec{k}}{(2\pi)^3}\,[U_k^E(\eta)e^{i\vec{k}\cdot\vec{x}}a_{\vec{k}}^E+U_k^{E*}(\eta)e^{-i\vec{k}\cdot\vec{x}}a_{\vec{k}}^{E\dagger}]. \tag{2.4}$$

With the commutator normalized to be

$$[a_{\vec{k}}^E,a_{\vec{k}'}^{E\dagger}]=(2\pi)^3\delta^3(\vec{k}-\vec{k}'), \tag{2.5}$$

the Euclidean Wightman function in position space is

$$\begin{aligned}G_E(x,x')&=\int\frac{d^3\vec{k}}{(2\pi)^3}\,e^{i\vec{k}\cdot(\vec{x}-\vec{x}')}U_k^E(\eta)U_k^{E*}(\eta')\\&\equiv\int\frac{d^3\vec{k}}{(2\pi)^3}\,e^{i\vec{k}\cdot(\vec{x}-\vec{x}')}G_k^E(\eta,\eta'),\end{aligned} \tag{2.6}$$

where the momentum representation the Wightman function is

$$G_k^E(\eta,\eta')=U_k^E(\eta)U_k^{E*}(\eta'). \tag{2.7}$$

Note that the mode functions only depend on the magnitude of the spatial momentum, $k=|\vec{k}|$.

A free massive scalar field satisfies the Klein-Gordon equation,

$$[\nabla^2+m^2]\Phi(x)=0, \tag{2.8}$$

so that the mode functions solve the differential equation,

$$[\eta^2\partial_\eta^2-2\eta\partial_\eta+\eta^2k^2+m^2H^{-2}]U_k^E(\eta)=0. \tag{2.9}$$

Note that m^2 here represents the effective mass of the theory which includes any contribution from coupling the field to the curvature, Φ^2R. In de Sitter space-time the curvature R is constant so this coupling is of the same form as a mass term. The solutions to Eq. (2.9) are linear combinations of Bessel functions,

$$U_k^E(\eta)=c_k\eta^{3/2}J_\nu(k\eta)+d_k\eta^{3/2}Y_\nu(k\eta), \tag{2.10}$$

with

$$\nu=\sqrt{\tfrac{9}{4}-m^2H^{-2}}. \tag{2.11}$$

We shall assume hereafter that ν is real.

The general form for the mode functions is applicable to both the Euclidean vacuum and the α-vacuum. What distinguishes the former is that as the Hubble constant is taken to vanish, $H\to 0$, so that de Sitter space becomes flat, we should recover only the positive frequency mode functions, e^{-ikt}. In the small H limit,

$$k\eta\to-\frac{ke^{-Ht}}{H}=-\frac{k}{H}+kt+\mathcal{O}(H), \tag{2.12}$$

the leading time dependence of the modes is $U_k^E(\eta)\propto e^{-ikt}$ when

$$c_k=N_k \qquad d_k=-iN_k. \tag{2.13}$$

Up to the normalization factor, N_k, the Euclidean mode functions are given by

$$\begin{aligned} U_k^E(\eta)&=N_k\eta^{3/2}[J_\nu(k\eta)-iY_\nu(k\eta)]\\ &=N_k\eta^{3/2}H_\nu^{(2)}(k\eta). \end{aligned} \tag{2.14}$$

$H_\nu^{(2)}(k\eta)$ represents a Hankel function. We shall now choose the units such that $H=1$.

The normalization is fixed by the canonical equal-time commutation relation

$$[\Pi(\eta,\vec{x}),\Phi(\eta,\vec{x}')]=-i\delta^3(\vec{x}-\vec{x}') \tag{2.15}$$

where the conjugate momentum is

$$\Pi(\eta,\vec{x})=\frac{1}{\eta^2}\partial_\eta\Phi(\eta,\vec{x}). \tag{2.16}$$

The equal-time commutation relation requires that the modes satisfy a Wronskian condition of the form

$$U_k^E\partial_\eta U_k^{E*}-\partial_\eta U_k^E U_k^{E*}=i\eta^2, \tag{2.17}$$

which determines the normalization of the modes to be

$$N_k=\frac{\sqrt{\pi}}{2}. \tag{2.18}$$

Therefore, the Euclidean mode functions are given by

$$U_k^E(\eta)=\frac{\sqrt{\pi}}{2}\eta^{3/2}H_\nu^{(2)}(k\eta). \tag{2.19}$$

While the de Sitter invariance of the Wightman function is not manifest from Eq. (2.19), it is possible to write $G_E(x,x')$ as a function of the de Sitter invariant distance between its arguments [24]. In conformally flat coordinates, this invariant distance between $x=(\eta,\vec{x})$ and $x'=(\eta',\vec{x}')$ is

$$Z(x,x')=\frac{\eta^2+\eta'^2-|\vec{x}-\vec{x}'|^2}{2\eta\eta'}. \tag{2.20}$$

Although we shall state most of our results in terms of the mode functions for a general mass, it will be convenient to show the results for a particular case in which the mode functions simplify substantially. When $\nu=\frac{1}{2}$, the Hankel function in Eq. (2.19) is proportional to an exponential,

$$U_k^E(\eta)|_{\nu=1/2}=\frac{i}{\sqrt{2k}}\eta e^{-ik\eta}. \tag{2.21}$$

This case corresponds to a massless, conformally coupled scalar field for which the effective mass is $m^2=2$. The Euclidean Wightman function is then

$$G_E(x,x')=\frac{\eta\eta'}{16\pi^3}\int\frac{d^3\vec{k}}{k}e^{-ik(\eta-\eta')}e^{i\vec{k}\cdot(\vec{x}-\vec{x}')} \tag{2.22}$$

and is finite provided we choose the appropriate $i\epsilon$ prescription,

$$G_E(x,x')=-\frac{1}{8\pi^2}\frac{1}{Z-1-i\epsilon\,\mathrm{sgn}(\eta-\eta')}. \tag{2.23}$$

Here the appearance of the invariant distance $Z(x,x')$ establishes the de Sitter invariance of the vacuum.

B. The α-vacua

The choice of the short distance behavior of the mode functions which determined the relative contributions of the two independent solutions to the Klein-Gordon equation is not the unique choice which leads to a de Sitter invariant Wightman function. Mottola [4] and Allen [5] observed that the vacuum state $|\alpha\rangle$ annihilated by a Bogolubov transformation of the Euclidean operators,

$$a_{\vec{k}}^\alpha=N_\alpha[a_{\vec{k}}^E-e^{\alpha*}a_{-\vec{k}}^{E\dagger}], \tag{2.24}$$

also yields a de Sitter invariant Wightman function,

$$G_\alpha(x,x')\equiv\langle\alpha|\Phi(x)\Phi(x')|\alpha\rangle. \tag{2.25}$$

Here, Re $\alpha<0$ and the normalization

$$N_\alpha = (1 - e^{\alpha+\alpha^*})^{-1/2} \tag{2.26}$$

is chosen to preserve the normalization of the commutation relation in the α-vacua, analogous to Eq. (2.5). Note that the Euclidean vacuum is itself among the α-vacua being obtained when $\alpha \to -\infty$.

In proving that $G_\alpha(x,x')$ only depends on $Z(x,x')$ it is useful to use a coordinatization that covers the entire de Sitter space-time. In such global coordinates, both a point x and its antipode x_A occur in the same coordinate system [24]. It is then possible to choose Euclidean mode functions $\phi_n^E(x)$ such that $\phi_n^{E*}(x) = \phi_n^E(x_A)$ so that the Bogolubov transformation of Eq. (2.24) gives

$$\phi_n^\alpha(x) = N_\alpha[\phi_n^E(x) + e^\alpha \phi_n^E(x_A)]. \tag{2.27}$$

Here n labels the elements of a general basis of mode functions. In this form, the de Sitter invariance of the Euclidean Wightman function and the fact that $Z(x,x_A') = -Z(x,x')$ together imply that the α-Wightman function only depends on the de Sitter invariant distance between x and x' [4,5]. While it is helpful to use a coordinate system which contains the antipode of every point to establish this invariance, for explicit calculations it is not necessary to use global coordinates. Equation (2.24) relates the mode functions of the α-vacuum to the mode functions of the Euclidean vacuum and their complex conjugates—we do not need to transform the conjugated mode function into a function of the antipode once we have established that $G_\alpha(x,x')$ is invariant.

From the Euclidean mode functions of Eq. (2.19) we can now construct the mode functions for the α-vacua. Expanding the scalar field in terms of α creation and annihilation operators,

$$\Phi(\eta,\vec{x}) = \int \frac{d^3\vec{k}}{(2\pi)^3}\ [U_k^\alpha(\eta) e^{i\vec{k}\cdot\vec{x}} a_{\vec{k}}^\alpha + U_k^{\alpha*}(\eta) e^{-i\vec{k}\cdot\vec{x}} a_{\vec{k}}^{\alpha\dagger}], \tag{2.28}$$

and using Eq. (2.24) yields

$$U_k^\alpha(\eta) = N_\alpha[U_k^E(\eta) + e^\alpha U_k^{E*}(\eta)] \tag{2.29}$$

since the $U_k^E(\eta)$ only depend on the magnitude of $\vec{k}$. Thus the α-vacuum modes are

$$U_k^\alpha(\eta) = N_\alpha \frac{\sqrt{\pi}}{2} \eta^{3/2} [H_\nu^{(2)}(k\eta) + e^\alpha H_\nu^{(1)}(k\eta)]. \tag{2.30}$$

Inserting the α-mode expansion into Eq. (2.25) yields

$$G_\alpha(x,x') = \int \frac{d^3\vec{k}}{(2\pi)^3}\ e^{i\vec{k}\cdot(\vec{x}-\vec{x}')} U_k^\alpha(\eta) U_k^{\alpha*}(\eta'). \tag{2.31}$$

Again, the spatial flatness makes it natural to use a momentum representation

$$G_k^\alpha(\eta,\eta') = U_k^\alpha(\eta) U_k^{\alpha*}(\eta'). \tag{2.32}$$

The additional complexity of the mode functions in the α-vacuum means that it is particularly helpful to have a case in which these functions simplify. For a massless, conformally coupled scalar field,

$$U_k^\alpha(\eta)\big|_{\nu=1/2} = N_\alpha \frac{i}{\sqrt{2k}} \eta [e^{-ik\eta} - e^\alpha e^{ik\eta}], \tag{2.33}$$

and the Wightman function becomes

$$\begin{aligned} G_\alpha(x,x') = -\frac{N_\alpha^2}{8\pi^2}\Bigg\{ & \frac{1}{Z-1-i\epsilon\,\mathrm{sgn}(\eta-\eta')} \\ & + \frac{e^{\alpha+\alpha^*}}{Z-1+i\epsilon\,\mathrm{sgn}(\eta-\eta')} \\ & - \frac{e^\alpha}{Z+1-i\epsilon} - \frac{e^{\alpha^*}}{Z+1+i\epsilon}\Bigg\}. \end{aligned} \tag{2.34}$$

As in the Euclidean case, the de Sitter invariance is manifest in the above expression.

C. Propagation

To study the propagation of signals in a de Sitter background, define the Feynman propagator,

$$-iG(x,x') \equiv \langle \alpha | T(\Phi(x)\Phi(x')) | \alpha \rangle, \tag{2.35}$$

so that it satisfies the Klein-Gordon equation with a point source,

$$[\nabla_x^2 + m^2] G(x,x') = \frac{\delta^4(x-x')}{\sqrt{-g(x)}}. \tag{2.36}$$

The propagator can only depend on the difference between the spatial positions of the points so that its Fourier transform is

$$G_k(\eta,\eta') = \int d^3\vec{x}\, e^{-i\vec{k}\cdot(\vec{x}-\vec{x}')} G(\eta,\vec{x};\eta',\vec{x}') \tag{2.37}$$

where $G_k(\eta,\eta')$ is the solution to

$$[\eta^2\partial_\eta^2 - 2\eta\partial_\eta + \eta^2 k^2 + m^2] G_k(\eta,\eta') = \eta^2 \eta'^2 \delta(\eta-\eta'). \tag{2.38}$$

The solution to this equation which satisfies the correct boundary conditions at $\eta' = \eta$ has the form

$$\begin{aligned} G_k(\eta,\eta') = {} & G_k^>(\eta,\eta')\Theta(\eta-\eta') \\ & + G_k^<(\eta,\eta')\Theta(\eta'-\eta). \end{aligned} \tag{2.39}$$

Here $G_k^>(\eta,\eta')$ and $G_k^<(\eta,\eta')$ are essentially the two-point Wightman functions calculated earlier in Eq. (2.32),

$$G_k^{>}(\eta,\eta') = iG_k^{\alpha}(\eta,\eta') = iU_k^{\alpha}(\eta)U_k^{\alpha *}(\eta')$$

$$G_k^{<}(\eta,\eta') = iG_k^{\alpha}(\eta',\eta) = iU_k^{\alpha *}(\eta)U_k^{\alpha}(\eta'). \tag{2.40}$$

Although propagation for a free field theory in the α-vacua contains some peculiar features, it is not otherwise ill-defined. The pathological features of quantum field theory in an α-vacuum only appear in an interacting field theory. The form of the α-Wightman function already suggests that the interacting theory could be ill-defined, since the various terms in Eq. (2.34) contain different $i\epsilon$ prescriptions. This property implies that in a standard approach to calculating the one loop corrections to the propagator, among the products of the propagators participating in the loop appear products of poles with the opposite $i\epsilon$ prescription—pinched singularities [21]. For example, in the one-loop correction to the propagator appears a product of the Green's functions given in Eq. (2.34). However, these pinched singularities do not by themselves prove whether the α-vacuum is itself pathological or whether the standard methods for studying the quantized theory are inappropriate for a time-evolving background such as de Sitter space.

III. THE SCHWINGER-KELDYSH FORMALISM

A significant difference between de Sitter space, in most coordinatizations, and flat space is the explicit time dependence of the metric. Unlike a flat space-time where the generator of time translations is a Killing vector globally, de Sitter space-time has no such global timelike Killing vector. Moreover, in a particular coordinate system—such as inflationary coordinates—the time derivative may not even generate an isometry locally. These properties suggest that rather than attempt to define an *S*-matrix between ''in'' and ''out'' states defined at different times, we should apply a quantization procedure that evolves an entire matrix element over a finite interval. It is also useful to be able to evolve a given state forward from a specified initial time η_0, rather than to use a state in the asymptotic past. We can always take $\eta_0 \to -\infty$.

An additional advantage of solving the evolution over finite intervals is that such an approach more immediately determines whether the α-vacuum is applicable for inflation, which does not require a de Sitter space-time eternally, but only over a sufficient interval to generate the number of *e*-foldings needed to explain the flatness and the homogeneity of the universe. If the interacting α-vacuum shows its pathology even over a finite interval, then we can exclude the possibility that the universe was in a pure α-state during any epoch of inflation, regardless of the prior history of the universe.

The closed time contour formalism developed by Schwinger [10], Keldysh [11] and Mahanthappa [26] allows us to study the evolution of a quantum field theory over a finite interval after specifying the state at an initial surface. We review here their approach which leads to an expression for perturbatively evaluating the matrix element of an operator, which is given at the end of this section in Eq. (3.15).

In the interaction picture, the evolution of operators is given by the free Hamiltonian, H_0, while the evolution of states is given by the interactions, H_I. If we let $\{|\Psi\rangle\}$ denote a general basis of states for the theory, then the behavior of the system is completely described by the density matrix, $\rho(\eta) = \Sigma_{\Psi,\Psi'}\,\rho_{\Psi,\Psi'}|\Psi\rangle\langle\Psi'|$. Thus, as the density matrix is constructed from the states, it satisfies a Schrödinger equation of the form

$$i\frac{\partial}{\partial\eta}\rho(\eta) = [H_I,\rho(\eta)]. \tag{3.1}$$

The advantage of the interaction picture is that fields evolve using the free Hamiltonian,

$$-i\frac{\partial}{\partial\eta}\Phi(\eta,\vec{x}) = [H_0,\Phi(\eta,\vec{x})]. \tag{3.2}$$

The time evolution of the field is precisely that given in the previous section since here the mode functions still are solutions to the free Klein-Gordon equation.

To study the evolution introduced by the interactions, it is convenient to include a ''turning on'' function in the interacting part of the Hamiltonian,

$$H = H_0 + \omega(\eta-\eta_0)H_I. \tag{3.3}$$

Here $\omega(\eta-\eta_0)$ vanishes when $\eta<\eta_0$ and becomes one when η is sufficiently large compared with η_0. Later we shall let this function be a Θ step function. We shall often not write this function explicitly, absorbing it into H_I. Thus the state does not evolve before η_0: $\rho(\eta)=\rho(\eta_0)\equiv\rho_0$ for $\eta<\eta_0$.

Once we have specified the state at a particular time, $\rho(\eta_0)$, then the Eq. (3.1) allows us to determine the state at all subsequent times. To study the vacuum structure of de Sitter space, the initial state will correspond to an α-vacuum. If we introduce a unitary, time-evolution operator $U_I(\eta,\eta')$ that evolves the state,

$$\rho(\eta) = U_I(\eta,\eta_0)\rho(\eta_0)U_I^{-1}(\eta,\eta_0), \tag{3.4}$$

then from Eq. (3.1) $U(\eta,\eta_0)$ obeys

$$i\frac{\partial}{\partial\eta}U_I(\eta,\eta_0) = H_I U_I(\eta,\eta_0) \tag{3.5}$$

with $U_I(\eta_0,\eta_0)=1$. The formal solution to this equation is given by Dyson's equation in terms of the time-ordered exponential

$$U_I(\eta,\eta_0) = Te^{-i\int_{\eta_0}^{\eta} d\eta''\, H_I(\eta'')}. \tag{3.6}$$

The evolution of the expectation value of an operator in this time-dependent background is given by

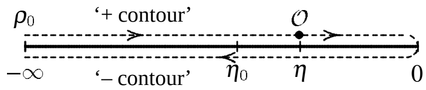

FIG. 1. The contour used to evaluate the evolution of operators over a finite time interval. The initial state is an eigenstate of the Hamiltonian until η_0 at which time the interactions are turned on. We double the field content so that separate copies of the fields are used for the upper and lower parts of the contour.

$$\langle\mathcal{O}\rangle(\eta)=\frac{\mathrm{Tr}[\rho(\eta)\mathcal{O}]}{\mathrm{Tr}[\rho(\eta)]}=\frac{\mathrm{Tr}[\rho_0 U_I^{-1}(\eta,\eta_0)\mathcal{O}U_I(\eta,\eta_0)]}{\mathrm{Tr}[\rho_0]}. \tag{3.7}$$

Since the state $\rho(\eta_0)$ does not evolve before the interactions are turned on, we can insert the identity in the form $U_I(\eta_0,\eta_p)U_I(\eta_p,\eta_0)$ with $\eta_p<\eta_0$ and commute one of these evolution operators with ρ_0 to obtain

$$\langle\mathcal{O}\rangle(\eta)=\frac{\mathrm{Tr}[\rho_0 U_I(\eta_p,\eta)\mathcal{O}U_I(\eta,\eta_p)]}{\mathrm{Tr}[\rho_0]}. \tag{3.8}$$

Inserting another factor of the identity, $U_I(\eta_p,\eta_f)U_I(\eta_f,\eta_p)$, with $\eta_f>\eta$ yields

$$\langle\mathcal{O}\rangle(\eta)=\frac{\mathrm{Tr}[\rho_0 U_I(\eta_p,\eta_f)U_I(\eta_f,\eta)\mathcal{O}U_I(\eta,\eta_p)]}{\mathrm{Tr}[\rho_0]} \tag{3.9}$$

and finally we let $\eta_p\to-\infty$ and $\eta_f\to 0$, which represent the infinite past and infinite future in conformal coordinates, so that

$$\langle\mathcal{O}\rangle(\eta)=\frac{\mathrm{Tr}[U_I(-\infty,0)U_I(0,\eta)\mathcal{O}U_I(\eta,-\infty)\rho_0]}{\mathrm{Tr}[U_I(-\infty,0)U_I(0,-\infty)\rho_0]}. \tag{3.10}$$

Reading the operators from right to left in the numerator of this equation, ρ_0 sets the initial state of the system which is then evolved along a time contour from $-\infty$ to 0 with an operator inserted at η; the final operator evolves back from 0 to $-\infty$. The closed time contour which results is depicted in Fig. 1.

To evaluate Eq. (3.10) it is useful to group the evolution operators into a single time-ordered exponential. This is accomplished by formally doubling the field content of the theory, with a set of "+" fields on the increasing-time contour and a set of "−" fields on the decreasing-time contour. The arrows on the contour indicate time ordering of events so that events on the − contour always occur after those on the + contour. We can group the effects of both parts of the contour together by writing the interacting part of the action appearing in Dyson's equation, as

$$S_I=-\int_{-\infty}^{0}d\eta\, H_I(\Phi^+)-\int_{0}^{-\infty}d\eta\, H_I(\Phi^-). \tag{3.11}$$

Since the two terms differ only in the direction of the integral over the conformal time, we can write the action as a single Lagrange density,

$$S_I=-\int_{-\infty}^{0}d\eta\,[H_I(\Phi^+)-H_I(\Phi^-)]. \tag{3.12}$$

The field doubling induced by the closed contour effectively doubles the number of vertices we must include when studying any process—one set with fields on the + branch and one with fields on the − branch. From Eq. (3.12), the latter will have couplings with the opposite sign. In evaluating matrix elements, Wick contractions produce four propagators for the possible contractions of pairs of the two types of fields,

$$\langle\alpha|T(\Phi^{\pm}(\eta,\vec{x})\Phi^{\pm}(\eta',\vec{x}'))|\alpha\rangle=-i\int\frac{d^3\vec{k}}{(2\pi)^3}\;e^{i\vec{k}\cdot(\vec{x}-\vec{x}')}G_k^{\pm\pm}(\eta,\eta'). \tag{3.13}$$

The time-ordering of the contractions is determined by the direction along the contour,

$$\begin{aligned}
G_k^{++}(\eta,\eta')&=G_k^{>}(\eta,\eta')\Theta(\eta-\eta')+G_k^{<}(\eta,\eta')\Theta(\eta'-\eta)\\
G_k^{--}(\eta,\eta')&=G_k^{>}(\eta,\eta')\Theta(\eta'-\eta)+G_k^{<}(\eta,\eta')\Theta(\eta-\eta')\\
G_k^{-+}(\eta,\eta')&=G_k^{>}(\eta,\eta')\\
G_k^{+-}(\eta,\eta')&=G_k^{<}(\eta,\eta'),
\end{aligned} \tag{3.14}$$

with the Wightman functions given in Eq. (2.40).

Assembling the ingredients of the Schwinger-Keldysh formalism—the general expression for an operator expectation value in Eq. (3.10), Dyson's equation (3.6) and Eq. (3.12)—provides an explicit expression for the evolution of $\langle\mathcal{O}\rangle(\eta)$. If we let the initial density matrix be that for a pure α-vacuum, then Eq. (3.10) becomes

$$\langle\alpha|\mathcal{O}|\alpha\rangle(\eta)=\frac{\langle\alpha|T\{\mathcal{O}_I e^{-i\int_{-\infty}^{0}d\eta\,[H_I(\Phi^+)-H_I(\Phi^-)]}\}|\alpha\rangle}{\langle\alpha|T\{e^{-i\int_{-\infty}^{0}d\eta\,[H_I(\Phi^+)-H_I(\Phi^-)]}\}|\alpha\rangle}. \tag{3.15}$$

Here we have absorbed any "turning on" function in H_I—in essence the time integrals begin at η_0. The time ordering has allowed us to group the time evolution operators in Eq. (3.10) along the two contours into a single operator. This equation for the finite evolution of the expectation value of $\mathcal{O}$ is the analogue of the standard S-matrix expression used in Minkowski space. The virtue of the field doubling is that it removes any acausal behavior from the matrix element since the Θ functions in the propagators combine to limit the upper end of the conformal time integrals to η [10,11]. This property will become clear in the calculation of a specific example.

IV. EVOLUTION OF THE NUMBER OPERATOR

We now evaluate the expectation value of the number of Euclidean particles in the α-vacuum using the Schwinger-Keldysh formalism [27]. This number operator provides a good measure of whether a particular choice for the vacuum state becomes pathological in the presence of interactions. From the perspective of the Euclidean vacuum, the α-vacuum is an excited state. We can determine the stability of this state when the interactions are turned on by following the time evolution of the change in the Euclidean number operator evaluated in the α-vacuum.

In the noninteracting theory, we should not encounter any infinite Euclidean particle production in the α-vacuum. When the interactions are turned on, some further particle production will occur in the Euclidean vacuum, but the rate per unit volume should be finite and any divergences which appear perturbatively must be renormalizable. What we shall discover is that in the interacting theory, the α-vacuum produces a new class of divergences that cannot be removed with the usual set of counterterms.

These divergences in the α-vacuum occur at each time in the integrand as we propagate from some initial state at η_0 to a finite time later so that the theory diverges even for an arbitrarily short time after the interactions are turned on. This behavior indicates that the α-vacuum is inappropriate even for a finite inflationary epoch.

Although we examine in detail the evolution of the Euclidean number operator in this section, all of the divergences we find are generic to the one loop corrections to an arbitrary operator. Furthermore, while we consider a scalar theory with a cubic interaction since it has a simple, nontrivial self-energy correction, similar loop integrals occur in any interacting scalar field theory. These more general cases are treated in the next section.

We first show how the free Hamiltonian can produce a nontrivial, but finite, time dependence. We then set up the calculation for the expectation value of the derivative of the number operator, expressing it in terms of the scalar field and its conjugate momentum. The corrections to this expectation value to leading, nontrivial order in the coupling are then calculated and we obtain general expressions for the one-loop corrections and the counterterms.

In the interaction picture, the Hamiltonian is divided into free and interacting parts,

$$H=H_0+\Theta(\eta-\eta_0)H_I. \tag{4.1}$$

Here we have included a Θ function so that before η_0 the system evolves freely; we are always free to take $\eta_0\to-\infty$. For conformally flat de Sitter coordinates, the free Hamiltonian for a scalar field $\Phi(\eta,\vec{x})$ of mass m is given by

$$H_0=\int d^3\vec{x}\big[\tfrac{1}{2}\eta^2\Pi^2+\tfrac{1}{2}\eta^{-2}(\vec{\nabla}\Phi)^2+\tfrac{1}{2}\eta^{-4}m^2\Phi^2\big]. \tag{4.2}$$

An important difference between de Sitter space and flat space is that the free Hamiltonian is not diagonal in terms of creation and annihilation operators,

$$\begin{aligned}H_0=\frac{1}{2}\frac{1}{\eta^2}\int\frac{d^3\vec{k}}{(2\pi)^3}\{&[a_{\vec{k}}^E a_{\vec{k}}^{E\dagger}+a_{\vec{k}}^{E\dagger}a_{\vec{k}}^E]g_k^E(\eta)\\&+a_{\vec{k}}^E a_{-\vec{k}}^E f_k^E(\eta)+a_{\vec{k}}^{E\dagger}a_{-\vec{k}}^{E\dagger}f_k^{E*}(\eta)\}\end{aligned} \tag{4.3}$$

where

$$g_k^E=\partial_\eta U_k^E\partial_\eta U_k^{E*}+\left[k^2+\frac{m^2}{\eta^2}\right]U_k^E U_k^{E*}$$

$$f_k^E=\partial_\eta U_k^E\partial_\eta U_k^E+\left[k^2+\frac{m^2}{\eta^2}\right]U_k^E U_k^E. \tag{4.4}$$

Note that this property holds also for the α-vacuum, $E\to\alpha$.

The origin of the off-diagonal terms in the free Hamiltonian lies in the fact that the surfaces of constant conformal time are not orthogonal to the generator of an isometry. This effect introduces an additional nontrivial source of time evolution which combines with that produced by the evolution of the state $|\alpha\rangle$ when the fields interact. For a time derivative of a generic operator, we formally have

$$\begin{aligned}\partial_\eta\langle\mathcal{O}(\eta)\rangle&=\mathrm{Tr}[(\partial_\eta\rho)\mathcal{O}+\rho\partial_\eta\mathcal{O}]\\&=i\,\mathrm{Tr}\big[-[H_I,\rho]\mathcal{O}+\rho[H_0,\mathcal{O}]\big]\\&=i\,\mathrm{Tr}\big[\rho[H,\mathcal{O}]\big]=i\langle[H,\mathcal{O}]\rangle.\end{aligned} \tag{4.5}$$

The off-diagonal terms in the free Hamiltonian induce an evolution in the number operator even in the free theory. Since we wish to explore the effect of interactions on the α-vacuum, we construct the number operator from creation and annihilation operators, $\tilde{a}_{\vec{k}}^\dagger$ and $\tilde{a}_{\vec{k}}$, which satisfy

$$\tilde{a}_{\vec{k}}(\eta_0)=a_{\vec{k}}^E \tag{4.6}$$

at the moment the interactions are turned on. The subsequent evolution in the interaction picture is given by the solution to

$$-i\frac{\partial}{d\eta}\tilde{a}_{\vec{k}}=[H_0,\tilde{a}_{\vec{k}}]. \tag{4.7}$$

The solution to this equation can be formally expressed as

$$\tilde{a}_{\vec{k}}(\eta)=U_0^{-1}(\eta,\eta_0)a_{\vec{k}}^E U_0(\eta,\eta_0) \tag{4.8}$$

where $U_0(\eta,\eta_0)$ is the time evolution operator for the free part of the theory,

$$U_0(\eta,\eta_0)=Te^{-i\int_{\eta_0}^{\eta}d\eta''H_0(\eta'')}. \tag{4.9}$$

From the form for the free Hamiltonian, a general solution to Eq. (4.7) is given by a Bogolubov transformation of the time independent creation and annihilation operators,

$$a_{\vec{k}}^E=\alpha_k(\eta)\tilde{a}_{\vec{k}}+\beta_k(\eta)\tilde{a}_{-\vec{k}}^\dagger, \tag{4.10}$$

where the coefficients satisfy

$$i\eta^2\partial_\eta\alpha_k^* = g_k^E\alpha_k^* + f_k^E\beta_k$$

$$-i\eta^2\partial_\eta\beta_k = g_k^E\beta_k + f_k^{E*}\alpha_k^* . \tag{4.11}$$

The standard normalization of the commutator of the transformed creation and annihilation operators also requires that

$$|\alpha_k(\eta)|^2 - |\beta_k(\eta)|^2 = 1. \tag{4.12}$$

The general solution to the coefficient equations (4.11) is of the form

$$\alpha_k^*(\eta) = a_1 U_k^E(\eta) + \frac{a_2}{\eta^2}\partial_\eta U_k^E(\eta)$$

$$\beta_k(\eta) = -a_1 U_k^{E*}(\eta) - \frac{a_2}{\eta^2}\partial_\eta U_k^{E*}(\eta) \tag{4.13}$$

where the constants a_1 and a_2 should satisfy

$$a_1 a_2^* - a_1^* a_2 = -i \tag{4.14}$$

from Eq. (4.12). If we would like the number operator to count the number of Euclidean particles at the moment we turn on the interactions, $\eta = \eta_0$, then

$$a_1 = -i\frac{\partial_\eta U_k^{E*}(\eta_0)}{\eta_0^2} \qquad a_2 = iU_k^{E*}(\eta_0). \tag{4.15}$$

The number operator constructed from the transformed creation and annihilation operators, $\tilde{a}_{\vec{k}}^\dagger \tilde{a}_{\vec{k}}$, has the correct evolution for an interaction picture operator. Using Eq. (4.5), even the free Hamiltonian induces some evolution in this number operator,

$$[H_0, \tilde{a}_{\vec{k}}^\dagger \tilde{a}_{\vec{k}}] = \frac{i}{\eta^4} D_{ab} \int d^3\vec{x}\, d^3\vec{y}\, e^{i\vec{k}\cdot(\vec{x}-\vec{y})}\Phi(\eta_a,\vec{x})\Phi(\eta_b,\vec{y}), \tag{4.16}$$

where $D_{ab}(\eta)$ is the differential operator,

$$D_{ab}(\eta) \equiv p_1(\eta)\partial_{\eta_a}\partial_{\eta_b} - p_2(\eta)(\partial_{\eta_a}+\partial_{\eta_b}) + p_3(\eta). \tag{4.17}$$

Here $\eta_{a,b}$ are only labels to indicate the functions on which the derivatives act; in the end, $\eta_{a,b}$ are set equal to η. The functions $p_i(\eta)$ are

$$p_1(\eta) = \frac{\eta^2}{\eta_0^2}\partial_\eta |U_k^E(\eta_0)|^2,$$

$$p_2(\eta) = \frac{\eta^4}{\eta_0^4}\; |\partial_\eta U_k^E(\eta_0)|^2 - \left[k^2 + \frac{m^2}{\eta^2}\right]|U_k^E(\eta_0)|^2$$

$$p_3(\eta) = -\frac{\eta^2}{\eta_0^2}\left[k^2 + \frac{m^2}{\eta^2}\right]\partial_\eta |U_k^E(\eta_0)|^2. \tag{4.18}$$

Evaluating Eq. (4.16) in the α-vacuum gives the tree level evolution of the number operator in this state,

$$i\langle\alpha|[H_0, \tilde{a}_{\vec{k}}^\dagger \tilde{a}_{\vec{k}}]|\alpha\rangle = -\frac{1}{\eta^4} V D_{ab}(\eta) U_k^\alpha(\eta_a) U_k^{\alpha*}(\eta_b). \tag{4.19}$$

V is the spatial volume. We can divide the volume from both sides to yield the particle production rate per unit volume for which this tree contribution is completely finite, if nonzero.

Now consider a cubic interaction with its associated counterterms,

$$H_I = \int d^3\vec{x}\, \eta^{-4}[J\Phi + \tfrac{1}{2}\delta m^2\Phi^2 + \tfrac{1}{3}\lambda\Phi^3]. \tag{4.20}$$

The cubic vertex will generally introduce one-loop corrections to the two-point functions, so we have included a mass counterterm, δm^2. Since the Φ^3 interaction breaks the $\Phi \to -\Phi$ symmetry of the free theory, we also expect the interaction to generate graphs containing tadpole insertions which are cancelled with the correct choice for J. To the order we shall study, no wave function renormalization is needed.

The change in the number operator induced by these interactions is given by applying Eq. (3.15),

$$\dot{N}_{\alpha,\vec{k}}^E(\eta) \equiv \frac{i\langle\alpha|T\{[H, \tilde{a}_{\vec{k}}^\dagger \tilde{a}_{\vec{k}}]e^{-i\int_{\eta_0}^0 d\eta [H_I(\Phi^+)-H_I(\Phi^-)]}\}|\alpha\rangle}{\langle\alpha|T\{e^{-i\int_{\eta_0}^0 d\eta [H_I(\Phi^+)-H_I(\Phi^-)]}\}|\alpha\rangle}. \tag{4.21}$$

The evolution of the free field is simple in the interaction picture, so it is useful to write the creation and annihilation operators in terms of the field and its conjugate momentum, by expanding in the time independent operators, Eq. (4.10), and inverting the operator expansion in Eq. (2.4),

$$a_{\vec{k}}^E = i\int d^3\vec{x}\, e^{-i\vec{k}\cdot\vec{x}}[U_k^{E*}\Pi(\eta,\vec{x}) - \eta^{-2}\partial_\eta U_k^{E*}\Phi(\eta,\vec{x})]$$

$$a_{\vec{k}}^{E\dagger} = -i\int d^3\vec{x}\, e^{i\vec{k}\cdot\vec{x}}[U_k^E\Pi(\eta,\vec{x}) - \eta^{-2}\partial_\eta U_k^E\Phi(\eta,\vec{x})]. \tag{4.22}$$

The commutator with the free part of the Hamiltonian is then as was given in Eq. (4.16) while that with the interacting part is

$$
\begin{aligned}
[H_I,\tilde{a}^{\dagger}_{\vec{k}}\tilde{a}_{\vec{k}}] = {}& \frac{i}{\eta^4}J(2\pi)^3\delta^3(\vec{k})\int d^3\vec{x}[2|U_k^E(\eta_0)|^2\Pi(\eta,\vec{x}) - \eta_0^{-2}\partial_\eta|U_k^E(\eta_0)|^2\Phi(\eta,\vec{x})] \\
& + \frac{i}{\eta^4}\delta m^2\int d^3\vec{x}d^3\vec{y}e^{i\vec{k}\cdot(\vec{x}-\vec{y})}[|U_k^E(\eta_0)|^2[\Phi(\eta,\vec{x})\Pi(\eta,\vec{y})+\Pi(\eta,\vec{x})\Phi(\eta,\vec{y})] \\
& - \eta_0^{-2}\partial_\eta|U_k^E(\eta_0)|^2\Phi(\eta,\vec{x})\Phi(\eta,\vec{y})] \\
& + \frac{i}{\eta^4}\frac{\lambda}{2}\int d^3\vec{x}d^3\vec{y}e^{i\vec{k}\cdot(\vec{x}-\vec{y})}[|U_k^E(\eta_0)|^2[\Phi^2(\eta,\vec{x})\Pi(\eta,\vec{y})+\Pi(\eta,\vec{x})\Phi^2(\eta,\vec{y})] \\
& - \eta_0^{-2}U_k^E(\eta_0)\partial_\eta U_k^{E*}(\eta_0)\Phi(\eta,\vec{x})\Phi^2(\eta,\vec{y}) - \eta_0^{-2}U_k^{E*}(\eta_0)\partial_\eta U_k^E(\eta_0)\Phi^2(\eta,\vec{x})\Phi(\eta,\vec{y})].
\end{aligned}
\tag{4.23}
$$

The expectation values of each of these commutators will be evaluated in the α-vacuum to order λ^2.

Before evaluating the expectation values of these commutators perturbatively, a large class of graphs, those containing a tadpole subgraph, are eliminated through the proper choice of the coefficient J of the linear counterterm. To leading order in λ, this choice for J is

$$J = -\frac{\lambda}{16\pi^3}\int d^3\vec{p}\ |U_p^\alpha(\eta'')|^2. \tag{4.24}$$

This cancellation is shown diagrammatically in Fig. 2. Note that while the loop integral in Eq. (4.24) contains an apparent time dependence, it is in fact time independent,

$$
\begin{aligned}
&\int d^3\vec{p}\ \ |U_p^\alpha(\eta'')|^2 \\
&\quad = N_\alpha^2\pi^2\int_0^\infty \xi^2 d\xi|H_\nu^{(2)}(\xi)+e^\alpha H_\nu^{(1)}(\xi)|^2.
\end{aligned}
\tag{4.25}
$$

The form of the leading corrections to the expectation value of $[H_I,\tilde{a}^{\dagger}_{\vec{k}}\tilde{a}_{\vec{k}}]$ in the α-vacuum are simpler since the commutator is already itself of order λ. The order λ^2 corrections to this commutator are shown diagrammatically in Fig. 3. The other corrections from the cubic interaction at this order contain tadpole subgraphs and are cancelled when Eq. (4.24) is satisfied.

One of the subtleties in evaluating the evolution of the number operator is that it contains time derivatives. For example, the δm^2 term of Fig. 3 contains a term of the form

$$\langle\alpha|T(\Phi(\eta,\vec{x})\Pi(\eta,\vec{y})+\Pi(\eta,\vec{x})\Phi(\eta,\vec{x}))|\alpha\rangle \tag{4.26}$$

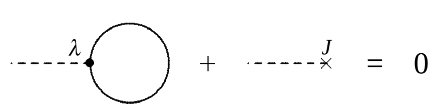

FIG. 2. The coefficient J of the linear counterterm is chosen to cancel insertions of tadpoles. The dashed line represents a line in a general diagram.

which can produce Schwinger terms if the time ordering of the operators is not treated carefully. A method for avoiding such terms, following [27], is to write the canonical momentum as

$$\Pi(\eta,\vec{x}) = \lim_{\eta''\to\eta}\frac{1}{\eta''^2}\partial_{\eta''}\Phi(\eta'',\vec{x}) \tag{4.27}$$

and then to place the fields on the appropriate contours so that the time ordering naturally given along the contour preserves the correct ordering of the operators in Eq. (4.26),

$$
\begin{aligned}
&\lim_{\eta''\to\eta}\frac{1}{\eta''^2}\partial_{\eta''}\langle\alpha|T(\Phi^-(\eta,\vec{x})\Phi^+(\eta'',\vec{y}) \\
&\qquad + \Phi^-(\eta'',\vec{x})\Phi^+(\eta,\vec{x}))|\alpha\rangle.
\end{aligned}
\tag{4.28}
$$

With this prescription, the mass counterterm in Fig. 3 contributes

$$
\begin{aligned}
\mathcal{C}_I = -\frac{\delta m^2}{\eta^6}V\Bigg\{&|U_k^E(\eta_0)|^2\partial_\eta|U_k^\alpha(\eta)|^2 \\
&-\frac{\eta^2}{\eta_0^2}\partial_\eta|U_k^E(\eta_0)|^2|U_k^\alpha(\eta)|^2\Bigg\}
\end{aligned}
\tag{4.29}
$$

at lowest order.

The only nontrivial effect of the interactions on expectation value of the commutator with the interaction Hamiltonian arises from the self-energy graph,

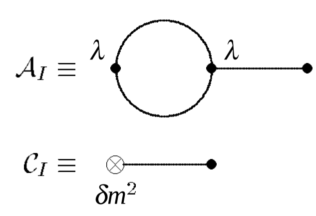

FIG. 3. After choosing the linear term to cancel graphs containing a tadpole, only these terms contribute at order λ^2 to the expectation value of $[H_I,\tilde{a}^{\dagger}_{\vec{k}}\tilde{a}_{\vec{k}}]$ in the α-vacuum. The first represents a self-energy graph while the second is from the mass counterterm.

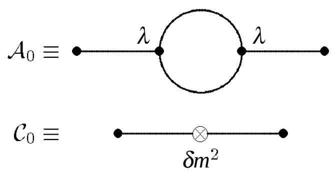

FIG. 4. The order λ^2 corrections to the expectation value of $[H_0, a_{\vec{k}}^{E\dagger} a_{\vec{k}}^{E}]$ in the α-vacuum. Again, the first represents a self-energy graph while the second is from the mass counterterm.

$$
\begin{aligned}
\mathcal{A}_I = & -\frac{\lambda^2}{\eta^6}\frac{V}{4\pi^3}|U_k^E(\eta_0)|^2 \\
& \times \int_{\eta_0}^{\eta} \frac{d\eta'}{\eta'^4}\ \mathrm{Im}[\partial_\eta U_k^\alpha(\eta) U_k^{\alpha *}(\eta') L_k^\alpha(\eta,\eta')] \\
& + \frac{\lambda^2}{\eta^4}\frac{V}{8\pi^3}\frac{\partial_\eta |U_k^E(\eta_0)|^2}{\eta_0^2} \\
& \times \int_{\eta_0}^{\eta} \frac{d\eta'}{\eta'^4}\ \mathrm{Im}[U_k^\alpha(\eta) U_k^{\alpha *}(\eta') L_k^\alpha(\eta,\eta')]
\end{aligned} \tag{4.30}
$$

where the loop integral is given by

$$
L_k^\alpha(\eta,\eta') \equiv \int d^3\vec{p}\, U_p^\alpha(\eta) U_p^{\alpha *}(\eta') U_{p-k}^\alpha(\eta) U_{p-k}^{\alpha *}(\eta'). \tag{4.31}
$$

In addition to the corrections in Eq. (4.29) and Eq. (4.30), the fact that the free Hamiltonian is not the conserved quantity associated with a timelike generator of an isometry of de Sitter space means that the expectation value of $[H_0, \tilde{a}_{\vec{k}}^{\dagger} \tilde{a}_{\vec{k}}]$ also contributes at order λ^2. The linear counterterm also cancels the graphs containing a tadpole subgraph and any vacuum to vacuum disconnected graphs are removed by the denominator of Eq. (4.21). The only remaining corrections then are those shown in Fig. 4. These graphs contribute

$$
\begin{aligned}
\mathcal{A}_0 = & -\frac{\lambda^2}{\eta^4}\frac{V}{2\pi^3} D_{ab}(\eta) \\
& \times \int_{\eta_0}^{\eta} \frac{d\eta_1}{\eta_1^4} \int_{\eta_0}^{\eta_1} \frac{d\eta_2}{\eta_2^4} \mathrm{Im}[U_k^\alpha(\eta_a) U_k^{\alpha *}(\eta_1)] \\
& \times \mathrm{Im}[U_k^\alpha(\eta_b) U_k^{\alpha *}(\eta_2) L_k^\alpha(\eta_1,\eta_2)]
\end{aligned} \tag{4.32}
$$

and

$$
\begin{aligned}
\mathcal{C}_0 = & -\frac{2\,\delta m^2}{\eta^4} V D_{ab}(\eta) \int_{\eta_0}^{\eta} \frac{d\eta_1}{\eta_1^4} \mathrm{Im}[U_k^\alpha(\eta_a) U_k^{\alpha *}(\eta_1) \\
& \times U_k^\alpha(\eta_b) U_k^{\alpha *}(\eta_1)]
\end{aligned} \tag{4.33}
$$

to the expectation value of the derivative of the number operator, $\dot{N}_{\alpha,\vec{k}}^{E}$.

An important feature to note is that the mass counterterm insertions, in Eq. (4.29) and Eq. (4.33), do not vanish in the Euclidean limit; they are needed to cancel a logarithmic divergence in the corresponding self-energy diagrams.

A. Renormalizing the logarithmic divergence

The one loop corrections in the generic α-vacuum and in the Euclidean limit differ in their divergence structure. Both cases contain a logarithmic divergence which can be regularized and cancelled by the appropriate choice for the mass counterterm, δm^2. What distinguishes the general α-vacuum from the Euclidean vacuum is the appearance of an additional class of terms that diverge linearly in the loop momentum. This divergence cannot be renormalized. In this subsection, we summarize the renormalization of the logarithmic divergence for the case of the massless conformally coupled scalar field in the Euclidean vacuum. The detailed calculation for the α-vacuum is left for the Appendix.

Formally, the evolution of the Euclidean number operator to order λ^2 in the Euclidean vacuum is given by

$$
\begin{aligned}
\dot{N}_{E,\vec{k}}^{E}(\eta) = & -\frac{1}{\eta^4} V D_{ab}(\eta) U_k^E(\eta_a) U_k^{E*}(\eta_b) \\
& + \lim_{\alpha\to-\infty} [\mathcal{A}_I + \mathcal{C}_I + \mathcal{A}_0 + \mathcal{C}_0].
\end{aligned} \tag{4.34}
$$

The case of a massless, conformally coupled scalar field is most readily analyzed since the mode functions have a simple form given in Eq. (2.21). The tree contribution in this case is given by

$$
\frac{V}{2k^2\eta^3}\left[\frac{\eta^4}{\eta_0^4} + k^2\eta^2\frac{\eta^2}{\eta_0^2} + \frac{\eta}{\eta_0} - k^2\eta_0^2 - \frac{\eta_0^2}{\eta^2}\right] \tag{4.35}
$$

which is finite for $\eta \in [\eta_0, 0)$. The loop integral for $\nu = \frac{1}{2}$, which occurs in $\mathcal{A}_I$, is

$$
L_{k,\nu=1/2}^{E}(\eta,\eta') \equiv -\frac{i\pi}{2}\frac{(\eta\eta')^2}{\eta-\eta'} e^{-ik(\eta-\eta')}, \tag{4.36}
$$

so that

$$
\begin{aligned}
\mathcal{A}_I = & \frac{\lambda^2}{k^2}\frac{V}{32\pi^2}\left[\frac{\eta_0^2}{\eta^4} - \frac{1}{\eta_0\eta}\right]\int_{\eta_0}^{\eta}\frac{d\eta'}{\eta-\eta'}\cos 2k(\eta-\eta') \\
& -\frac{\lambda^2}{k}\frac{V}{32\pi^2}\frac{\eta_0^2}{\eta^3}\int_{\eta_0}^{\eta}\frac{d\eta'}{\eta-\eta'}\sin 2k(\eta-\eta').
\end{aligned} \tag{4.37}
$$

The corresponding counterterm is

$$
\mathcal{C}_I = -\frac{\delta m^2}{k^2}\frac{V}{2}\left[\frac{\eta_0^2}{\eta^5} - \frac{1}{\eta_0\eta^2}\right]. \tag{4.38}
$$

The second integral in Eq. (4.37) is completely finite at all times $\eta < 0$. The first integral, however, contains a logarithmic divergence at the upper end of the $d\eta'$ integration. This term can be regularized as described in the Appendix. The pole as the regularization is removed, $\epsilon \to 0$, is given by

$$\mathcal{A}_I = \frac{\lambda^2}{k^2}\frac{V}{32\pi^2}\left[\frac{\eta_0^2}{\eta^5} - \frac{1}{\eta_0\eta^2}\right]\frac{1}{\epsilon} + \text{finite}, \tag{4.39}$$

and is cancelled by choosing

$$\delta m^2 = \frac{1}{\epsilon}\frac{\lambda^2}{16\pi^2} \tag{4.40}$$

in Eq. (4.38). The analogous logarithmic divergence in $\mathcal{A}_0$ is cancelled by the counterterm $\mathcal{C}_0$.

The self-energy diagrams in the α-vacuum also contain a logarithmic divergence which can be removed by a suitable choice for the mass counterterm,

$$\delta m^2 = \frac{1}{\epsilon}\frac{\lambda^2}{16\pi^2}(1 + e^{\alpha+\alpha^*})N_\alpha^2, \tag{4.41}$$

which reduces to that for the Euclidean case in Eq. (4.40). The origin and regularization of this divergence is discussed more fully in the Appendix.

B. The linear divergence of the α-vacuum

Including the order λ^2 corrections, the derivative of the number of Euclidean particles in the α-vacuum is again given by the sum of the contributions shown in Fig. 3 and Fig. 4 as well as the tree level contribution of Eq. (4.19),

$$\begin{aligned}\dot{N}^E_{\alpha,\vec{k}}(\eta) = &-\frac{1}{\eta^4}VD_{ab}(\eta)U_k^\alpha(\eta_a)U_k^{\alpha *}(\eta_b)\\ &+ \mathcal{A}_I + \mathcal{C}_I + \mathcal{A}_0 + \mathcal{C}_0.\end{aligned} \tag{4.42}$$

Each self-energy graph contains a loop integral, Eq. (4.31). Unlike the Euclidean case which is completely finite once we have established an $i\epsilon$ prescription, the loop integral over α-mode functions diverges linearly in the spatial momentum. Introducing a bound Λ to remove the large momenta in the loop, $\int_0^\infty p^2\,dp\int d\Omega_2 \to \int_0^\Lambda p^2\,dp\int d\Omega_2$, assuming $\Lambda > |\vec{k}|$, the divergent part of Eq. (4.31) is

$$\begin{aligned}L_k^\alpha(\eta_1,\eta_2) = e^{\alpha+\alpha^*}N_\alpha^4\frac{2\pi\Lambda}{k}(\eta_1\eta_2)^2\Bigg[&\frac{\sin k(\eta_1-\eta_2)}{\eta_1-\eta_2}\\ &+\frac{\sin k(\eta_1+\eta_2)}{\eta_1+\eta_2}\Bigg] + \text{finite}.\end{aligned} \tag{4.43}$$

The appearance of the factor $e^{\alpha+\alpha^*}$ shows why such a divergent term does not arise in the Euclidean limit.

Unlike the logarithmic divergence, this divergence cannot be removed by a momentum independent value for δm^2. For example, the divergent piece of the self-energy graph in Fig. 3 is

$$\begin{aligned}\mathcal{A}_I = &-e^{\alpha+\alpha^*}N_\alpha^4\frac{\lambda^2}{k\eta^4}\frac{V\Lambda}{2\pi^2}|U_k^E(\eta_0)|^2\\ &\times\int_{\eta_0}^{\eta}\frac{d\eta'}{\eta'^2}\mathrm{Im}\,\{\partial_\eta U_k^E(\eta)U_k^{E*}(\eta')\}\\ &\times\left[\frac{\sin k(\eta-\eta')}{\eta-\eta'} + \frac{\sin k(\eta+\eta')}{\eta+\eta'}\right]\\ &+e^{\alpha+\alpha^*}N_\alpha^4\frac{\lambda^2}{k\eta^2}\frac{V\Lambda}{4\pi^2}\frac{\partial_\eta|U_k^E(\eta_0)|^2}{\eta_0^2}\\ &\times\int_{\eta_0}^{\eta}\frac{d\eta'}{\eta'^2}\mathrm{Im}\{U_k^E(\eta)U_k^{E*}(\eta')\}\\ &\times\left[\frac{\sin k(\eta-\eta')}{\eta-\eta'} + \frac{\sin k(\eta+\eta')}{\eta+\eta'}\right] + \cdots\end{aligned} \tag{4.44}$$

which cannot be cancelled by a momentum-independent choice for δm^2 in Eq. (4.29).

To observe this incompatibility of the momentum dependence of the divergences in the α-vacua loop corrections and the available counterterms, at least in the case of a massless, conformally coupled scalar field, it is sufficient to compare the limiting behavior in the external momentum of the loop corrections and the corresponding counterterms. In the $k = |\vec{k}| \to 0$ limit the divergent parts of both $\mathcal{A}_I$ and $\mathcal{A}_I$ scale as $k^{-1}\Lambda$. In contrast, the leading k dependence of the counterterms scale as k^{-2}, at least when α is real, which is required in any case for a $\mathcal{CPT}$ invariant theory [24]. Thus, no choice of δm^2, which does not depend on k, is possible such that $\mathcal{C}_I$ and $\mathcal{C}_0$ cancel the divergence in $\mathcal{A}_I$ and $\mathcal{A}_0$ as $\Lambda\to\infty$.

Note that the linear divergence is not present in the opposite quantity—the expectation value of the number of α-particles in the Euclidean vacuum. This quantity is given by expressions similar to those above except with the labels interchanged for the mode functions, $U_q^\alpha \leftrightarrow U_q^E$, and some of the α-dependent coefficients are slightly altered in Eqs. (4.29)–(4.33). The crucial difference is that the presence of the Euclidean states in Eq. (3.15) leads to Euclidean propagators so that in particular the loop integral is over Euclidean modes for which no linear divergence occurs.

V. DISCUSSION

The linear divergence that arises from the one loop corrections in the α-vacuum is a UV effect. At arbitrarily short distances there exists an interference of the positive and negative frequency modes which cancels the rapidly oscillating phases among some of the terms within the loop integral. Without such a cancellation, these phases could damp these high-momentum contributions through an appropriate $i\epsilon$ prescription. This interference of phases is a specific feature of the propagator in the α-vacuum and does not occur in the Euclidean case. In this section we shall discuss the origin of this divergence and determine the necessary conditions for it to arise.

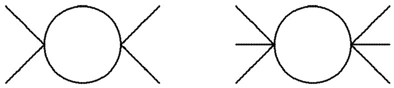

FIG. 5. Examples of divergent diagrams in theories with quartic (left) or quintic (right) interactions. Any loop that contains only two lines will exhibit a UV divergence similar to that in Eq. (4.43). This result follows from the structure of the propagator in the α-vacuum and not the form of the interactions.

Consider a loop containing n vertices connected by n internal propagators—those through which the common loop momentum flows. Since in de Sitter space it is convenient to perform a Fourier transform over only the spatial coordinates, each vertex has a time, η_i for $i=1,\ldots,n$, associated with it. Eventually, we integrate over all these times as they arise from the exponent of the time evolution operator in Eq. (3.15). To determine whether a particular loop can produce a UV divergence, we must first count the powers of momentum in the high loop momentum region.

Let $G^{>}_{p-k_i}(\eta_i,\eta_{i+1})$ represent the Wightman function within a loop propagator connecting the i and $(i+1)$ vertices. The loop momentum is $\vec{p}$ and $\vec{k}_i$ denotes other momenta following through the ith leg. In the UV limit $|\vec{p}-\vec{k}_i| \gg |\eta_i|^{-1},|\eta_{i+1}|^{-1}$, the leading behavior of this Wightman function is

$$G^{>}_{p-k_i}(\eta_i,\eta_{i+1}) \to iN_\alpha^2 \frac{\eta_i\eta_{i+1}}{2|\vec{p}-\vec{k}_i|}\left[e^{-i|\vec{p}-\vec{k}_i|(\eta_i-\eta_{i+1})} + e^{\alpha+\alpha^*}e^{i|\vec{p}-\vec{k}_i|(\eta_i-\eta_{i+1})} - ie^{\alpha}e^{-i\pi\nu}e^{i|\vec{p}-\vec{k}_i|(\eta_i+\eta_{i+1})} + ie^{\alpha^*}e^{i\pi\nu}e^{-i|\vec{p}-\vec{k}_i|(\eta_i+\eta_{i+1})}\right]. \quad (5.1)$$

Note that the propagator contains factors of both $G^{>}_{p-k_i}(\eta_i,\eta_{i+1})$ and $G^{<}_{p-k_i}(\eta_i,\eta_{i+1})=G^{>}_{p-k_i}(\eta_{i+1},\eta_i)$. For the purpose of the power counting, it is important to note that, aside from the phases, in the UV limit $G^{\alpha}_{p-k_i}(\eta_i,\eta_{i+1})\sim p^{-1}$. Thus in integrating over a loop,

$$\int^{\Lambda} d^3\vec{p}\prod_{i=1}^{n} G^{\alpha}_{p-k_i}(\eta_i,\eta_{i+1}) \sim \int^{\Lambda}\frac{dp}{p^{n-2}}. \quad (5.2)$$

We only encounter a possible UV divergence if $n\leqslant 3$. Note that the $n=1$ case can be removed by a counterterm since the loop only depends on the loop momentum and not on any other momenta in the graph.

The $n=2$ case can produce a linear divergence. Since the divergence only depends on the form of the propagator and not the form of the interaction, such divergences generically occur in any interacting theory, for example in the processes shown in Fig. 4 and Fig. 5. Superficially, a divergence might seem possible even in the Euclidean case if a product of Wightman functions, $G^{>}_{p}(\eta_1,\eta_2)G^{<}_{p-k}(\eta_1,\eta_2)$, occurs in the loop integral. However, the Schwinger-Keldysh formalism is constructed to remove such terms and only factors of $G^{>}_{p}(\eta_1,\eta_2)G^{>}_{p-k}(\eta_1,\eta_2)$, and $G^{<}_{p}(\eta_1,\eta_2)G^{<}_{p-k}(\eta_1,\eta_2)$ can appear in the loop integral in which the p-dependent phases do not cancel in the UV. The important difference in the α-vacuum is that each Wightman function contains terms whose p-dependent phases have the opposite signs. Thus even after the Schwinger-Keldysh formalism has been applied, a product of the two loop Green's functions,

$$G^{>}_{p}(\eta_1,\eta_2)G^{>}_{p-k}(\eta_1,\eta_2) \to -e^{\alpha+\alpha^*}N_\alpha^4\frac{(\eta_1\eta_2)^2}{4p|\vec{p}-\vec{k}|}\left[e^{-ip(\eta_1-\eta_2)}e^{i|\vec{p}-\vec{k}|(\eta_1-\eta_2)} + e^{ip(\eta_1-\eta_2)}e^{-i|\vec{p}-\vec{k}|(\eta_1-\eta_2)} + e^{ip(\eta_1+\eta_2)}e^{-i|\vec{p}-\vec{k}|(\eta_1+\eta_2)} + e^{-ip(\eta_1+\eta_2)}e^{i|\vec{p}-\vec{k}|(\eta_1+\eta_2)}\right]+\cdots \quad (5.3)$$

will have some phase cancellation as $p\to\infty$. What renders these terms unrenormalizable, however, is that although the p-dependent phases cancel in the divergent terms, they still contain a nontrivial dependence on the momentum entering the loop from the rest of the diagram.

This analysis of the phase structure of the two-propagator loop does not necessarily show that such divergences cannot be removed from the theory through a suitable renormalization prescription. This fact can only be established by summing all the contributions to this graph and demonstrating that the dependence of the resulting divergent term on the momenta external to the loop is incompatible with a counterterm insertion, as was done in the previous section. However, since all loop integrals containing only two propagators have essentially the same structure, given by Eq. (4.31), we see that the α-vacuum cannot be renormalized in any interacting theory, regardless of the form of the interaction.

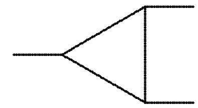

FIG. 6. Diagrams containing a loop with three propagators can be logarithmically divergent in the loop momentum. For example, a vertex correction in a Φ^3 theory could generate such a divergence.

The power counting argument indicates that a logarithmic divergence can arise for a loop with three legs, such as the vertex correction graph shown in Fig. 6. The loop integral contains a product of three terms of the form of Eq. (5.1), or its complex conjugate, which generally contains terms where the high loop momentum dependence of the phase cancels. For example, in Fig. 6 if the coordinates associated with the three vertices are $(\eta_1,\vec{k}_1)$, $(\eta_2,\vec{k}_2)$ and $(\eta_3,-\vec{k}_1-\vec{k}_2)$, then in the product of three propagators occur terms such as

$$G^{>}_{p-k_1}(\eta_1,\eta_2)G^{>}_{p+k_2}(\eta_2,\eta_3)G^{>}_{p}(\eta_1,\eta_3) \to -ie^{\alpha+\alpha^*}N_\alpha^6\frac{(\eta_1\eta_2\eta_3)^2}{8p|\vec{p}-\vec{k}_1||\vec{p}+\vec{k}_2|} \times e^{-i|\vec{p}-\vec{k}_1|(\eta_1-\eta_2)}e^{-i|\vec{p}+\vec{k}_2|(\eta_2-\eta_3)}e^{-ip(\eta_3-\eta_1)}+\cdots. \quad (5.4)$$

In the high momentum region of the loop momentum, the phase factor will be independent of the integrated momentum and the integral will be logarithmically divergent. As with the self-energy case before, these arguments can only demonstrate under what conditions a divergence can occur. Whether these logarithmic terms cancel among each other or whether the resulting divergence can be removed by a counterterm requires performing the full integration and summing all the relevant products of Wightman functions. However, since we have already seen that the self-energy graphs exhibit a pathological behavior in the α-vacuum, we shall not study these vertex corrections further here.

VI. CONCLUSIONS

The preceding discussion shows that a class of linear divergences from loops with two propagators—and logarithmic divergences from loops with three propagators—generically appears in any interacting theory in an α-vacuum. These divergences arise from the form of the α-vacuum propagator, which is determined by the free field Hamiltonian, and not on the detailed form of the interaction. What the Schwinger-Keldysh formalism allows is a precise statement of the problem of an interacting theory in an α-vacuum. With a high-momentum cutoff, we can find all the terms that diverge linearly with this cutoff and analyze their dependence on the momenta external to the loop. The resulting expressions are not cancelled by a set of de Sitter invariant counterterms of the same form as those in the original Lagrangian. The appearance of α-dependent prefactors also shows why such terms do not plague the Euclidean vacuum.

The fact that the divergence originates from high momentum modes and the form of the α-dependent prefactors provides the basis of a simple heuristic explanation for the divergence.[1] The number density of Euclidean particles per unit volume at the time that the interactions are turned on is

$$n_{\vec{k}}^{\alpha} \equiv V^{-1}\langle\alpha|a_{\vec{k}}^{E\dagger}a_{\vec{k}}^{E}|\alpha\rangle = e^{\alpha+\alpha^*}N_\alpha^2 = \frac{1}{e^{-\alpha-\alpha^*}-1} \tag{6.1}$$

since $\tilde{a}_{\vec{k}}(\eta_0)=a_{\vec{k}}^E$. From the perspective of the Euclidean vacuum, the α-vacuum looks like a distribution whose occupation number is given by $n_{\vec{k}}^{\alpha}$. Note that $n_{\vec{k}}^{\alpha}$ is actually independent of $\vec{k}$. If we then replace the α-dependent terms in the propagators with the factors $n_{\vec{k}}^{\alpha}$, maintaining the momentum labels, then among the many divergent terms contributing to $\mathcal{A}_I$ occurs the expression,

$$\begin{aligned}\mathcal{A}_I = -\frac{\lambda^2}{k\eta}\frac{V}{64\pi^3}\frac{\partial_\eta|U_k^E(\eta_0)|^2}{\eta_0^2}\int_{\eta_0}^{\eta}\frac{d\eta'}{\eta'}\int\frac{d^3\vec{p}}{p|\vec{p}-\vec{k}|}\\ \times[(n_{\vec{k}}^{\alpha}+1)(n_{\vec{p}}^{\alpha}+1)n_{\vec{p}-\vec{k}}^{\alpha}-n_{\vec{k}}^{\alpha}n_{\vec{p}}^{\alpha}(n_{\vec{p}-\vec{k}}^{\alpha}+1)]\\ \times\sin[[p+k-|\vec{p}-\vec{k}|](\eta-\eta')]+\cdots,\end{aligned} \tag{6.2}$$

in the massless conformally coupled case. This expression resembles a "gain minus loss" process in the α background—for example, one part describes the creation of two particles from one while the other describes the creation of one from the annihilation of two. Since $n_{\vec{p}}^{\alpha}$ is constant, nothing suppresses the large p divergence.

This divergence is only present in a true α-vacuum and not in a "truncated α-vacuum"—a state that is set equal to a Euclidean vacuum above some scale $|\vec{k}|>M$ [12]. For a truncated α-vacuum, the $n_{\vec{p}}^{\alpha}$'s vanish above M so integrals such as Eq. (6.2) become finite. The largest contribution to the change in the number operator scales as $\lambda^2 M$. These truncated α-vacua have no divergences, although exactly how the state evolves may depend on how the truncation is implemented. Using our formalism, it becomes possible to study how one of these vacua evolves during inflation and the amount by which it would alter the appearance of angular power spectrum of the cosmic microwave background radiation [19].

To conclude then, interactions destabilize the α-vacua. We have calculated a physical quantity, the conformal time rate of change of the number of Euclidean mode particles in the α-vacuum, and found that it diverges. This divergence reflects a physical pathology of an interacting theory in a true α-vacuum.

ACKNOWLEDGMENTS

This work was supported in part by DOE grant DE-FG03-91-ER40682. We are grateful to Dan Boyanovsky for helpful discussions. R.H. thanks M. Einhorn, F. Larsen and Jim Cline for helpful discussions, as well as the Aspen Center for Physics where this work was begun.

APPENDIX: REGULARIZATION OF LOGARITHMIC DIVERGENCES

The self-energy diagrams in Fig. 3 and Fig. 4 contain two classes of divergences in the α-vacuum. One class diverges linearly in the magnitude of the spatial loop momentum. The dependence of this divergence on the external momentum flowing through the graph is not of the same form as that appearing from the insertion of one of the available counterterms. In this sense, these divergences cannot be renormalized and indicate a pathological feature of an interacting theory in the α-vacuum. However, these linearly divergent terms vanish in the Euclidean limit.

The second class of divergences exist in both the Euclidean and the general α-vacua. These divergences depend logarithmically on the conformal time and can, at least in the massless conformally coupled case where the calculation simplifies, be removed by a constant mass counterterm. It is important to establish the renormalization of this type of divergence not only to show that the evolution of the number operator is finite for an interacting scalar field in the Euclidean vacuum, but also in the α-case. If we wish to consider a "truncated α-vacuum," one which is cut off at some high energy scale such as the Planck mass [12], we thereby re-

[1] We would like to thank Dan Boyanovsky for suggesting this kinetic interpretation.

move the linear divergence of Eq. (4.43), but the logarithmic divergence is still present in $\mathcal{A}_I$ and $\mathcal{A}_0$. In this appendix, we demonstrate how to renormalize this divergence.

In the massless conformally coupled case, the loop integral over α-vacuum propagators of Eq. (4.31) yields

$$\begin{aligned}L^{\alpha}_{k,\nu=1/2}(\eta_1,\eta_2) = &-\frac{i\pi}{2}N_\alpha^2(\eta_1\eta_2)^2\frac{e^{-ik(\eta_1-\eta_2)}+e^{\alpha+\alpha^*}e^{ik(\eta_1-\eta_2)}}{\eta_1-\eta_2}\\ &+\frac{i\pi}{2}N_\alpha^4(\eta_1\eta_2)^2[e^\alpha-e^{\alpha^*}]\frac{e^\alpha e^{ik(\eta_1+\eta_2)}+e^{\alpha^*}e^{-ik(\eta_1+\eta_2)}}{\eta_1+\eta_2}\\ &-\frac{i\pi}{k}e^\alpha N_\alpha^4\eta_1\eta_2\sin k\eta_1[e^{ik\eta_2}-e^{2\alpha^*}e^{-ik\eta_2}]\\ &+\frac{i\pi}{k}e^{\alpha^*}N_\alpha^4\eta_1\eta_2\sin k\eta_2[e^{-ik\eta_1}-e^{2\alpha}e^{2ik\eta_1}]\\ &+\frac{2\pi}{k}(\Lambda-k)e^{\alpha+\alpha^*}N_\alpha^4(\eta_1\eta_2)^2\left[\frac{\sin k(\eta_1-\eta_2)}{\eta_1-\eta_2}+\frac{\sin k(\eta_1+\eta_2)}{\eta_1+\eta_2}\right].\end{aligned}\tag{A1}$$

The final term is the linearly divergent term. Among the remaining terms, only the first produces any logarithmic divergence when integrated over the conformal time. In the case of either self-energy contribution, Eq. (4.30) or Eq. (4.32), we integrate η_2 from η_0 to η_1 ($\eta_1\to\eta$ for the $\mathcal{A}_I$ graph) and encounter a singularity from the $(\eta_1-\eta_2)$ denominator of imaginary part of the first term in Eq. (A1),

$$L^{\alpha}_{k,\nu=1/2}(\eta_1,\eta_2) = -\frac{i\pi}{2}(1+e^{\alpha+\alpha^*})N_\alpha^2(\eta_1\eta_2)^2\frac{\cos k(\eta_1-\eta_2)}{\eta_1-\eta_2}+\cdots.\tag{A2}$$

Inserting this result in the self-energy contributions yields

$$\begin{aligned}\mathcal{A}_I=&\frac{\lambda^2}{k\eta^4}\frac{V}{16\pi^2}(1+e^{\alpha+\alpha^*})N_\alpha^4|U_k^E(\eta_0)|^2\int_{\eta_0}^{\eta}\frac{d\eta'}{\eta'(\eta-\eta')}\cos k(\eta-\eta')\\ &\times\{(1+e^{\alpha+\alpha^*})\cos k(\eta-\eta')-(e^\alpha e^{ik(\eta+\eta')}+e^{\alpha^*}e^{-ik(\eta+\eta')})-ik\eta(e^\alpha e^{ik(\eta+\eta')}-e^{\alpha^*}e^{-ik(\eta+\eta')})\}\\ &-\frac{\lambda^2}{k\eta}\frac{V}{32\pi^2}(1+e^{\alpha+\alpha^*})N_\alpha^4\frac{\partial_\eta|U_k^E(\eta_0)|^2}{\eta_0^2}\int_{\eta_0}^{\eta}\frac{d\eta'}{\eta'(\eta-\eta')}\cos k(\eta-\eta')\\ &\times\{(1+e^{\alpha+\alpha^*})\cos k(\eta-\eta')-(e^\alpha e^{ik(\eta+\eta')}+e^{\alpha^*}e^{-ik(\eta+\eta')})\}+\cdots\end{aligned}\tag{A3}$$

and

$$\begin{aligned}\mathcal{A}_0=&-\frac{\lambda^2}{k^2\eta^4}\frac{V}{16\pi^2}(1+e^{\alpha+\alpha^*})N_\alpha^4D_{ab}(\eta)\int_{\eta_0}^{\eta}\frac{d\eta_1}{\eta_1}\int_{\eta_0}^{\eta_1}\frac{d\eta_2}{\eta_2}\ \eta_a\eta_b\frac{\cos k(\eta_1-\eta_2)}{\eta_1-\eta_2}\\ &\times\sin k(\eta_a-\eta_1)[(1+e^{\alpha+\alpha^*})\cos k(\eta_b-\eta_2)-e^\alpha e^{ik(\eta_b+\eta_2)}-e^{\alpha^*}e^{-ik(\eta_b+\eta_2)}]+\cdots.\end{aligned}\tag{A4}$$

In both of these equations, the ellipses indicate terms which do not diverge logarithmically in the conformal time.

Both Eq. (A3) and Eq. (A4) contain divergent integrals of the form

$$\int_{\eta_0}^{\eta_1}\frac{e^{2iq\eta_2}d\eta_2}{\eta_2(\eta_1-\eta_2)},\tag{A5}$$

where q is k, 0, or $-k$. Changing to a dimensionless variable,

$$r\equiv 1-\frac{\eta_2}{\eta_1},\tag{A6}$$

Eq. (A5) becomes

$$\int_{\eta_0}^{\eta_1}\frac{e^{2iq\eta_2}d\eta_2}{\eta_2(\eta_1-\eta_2)}=-\frac{e^{2iq\eta_1}}{\eta_1}\int_0^{1-\eta_0/\eta_1}\frac{e^{-2iq\eta_1 r}dr}{(r-1)r}.\tag{A7}$$

We can regularize this integral by inserting a factor of r^ϵ in the integrand and then extract the pole as $\epsilon\to0$,

$$\int_0^{1-\eta_0/\eta_1} \frac{e^{-2iq\eta_1 r} r^{\epsilon-1} dr}{r-1} = -\frac{1}{\epsilon} + \text{finite}. \tag{A8}$$

Thus,

$$\int_{\eta_0}^{\eta_1} \frac{e^{2iq\eta_2} d\eta_2}{\eta_2(\eta_1-\eta_2)} = \frac{e^{2iq\eta_1}}{\eta_1}\frac{1}{\epsilon} + \text{finite}. \tag{A9}$$

Applying this regularization to the self-energy graphs gives

$$\mathcal{A}_I = \frac{\lambda^2}{\eta^6}\frac{V}{16\pi^2}\frac{1}{\epsilon}(1+e^{\alpha+\alpha^*})N_\alpha^2\bigg[|U_k^E(\eta_0)|^2\partial_\eta|U_k^\alpha(\eta)|^2 - \frac{\eta^2}{\eta_0^2}\partial_\eta|U_k^E(\eta_0)|^2|U_k^\alpha(\eta)|^2\bigg] + \cdots \tag{A10}$$

and

$$\mathcal{A}_0 = \frac{2\lambda^2}{\eta^4}\frac{V}{16\pi^2}\frac{1}{\epsilon}(1+e^{\alpha+\alpha^*})N_\alpha^2 D_{ab}(\eta) \times \int_{\eta_0}^{\eta}\frac{d\eta_1}{\eta_1^4}\mathrm{Im}\{U_k^\alpha(\eta_a)U_k^{\alpha*}(\eta_1)U_k^\alpha(\eta_b)U_k^{\alpha*}(\eta_1)\} + \cdots. \tag{A11}$$

In deriving Eq. (A11) we have used the fact that the operator $D_{ab}(\eta)$ is symmetric in η_a and η_b. Both poles are removed by the appropriate mass counterterm graphs $\mathcal{C}_I$ and $\mathcal{C}_0$ given in Eq. (4.29) and Eq. (4.33), respectively, when

$$\delta m^2 = \frac{1}{\epsilon}\frac{\lambda^2}{16\pi^2}(1+e^{\alpha+\alpha^*})N_\alpha^2. \tag{A12}$$

---

[1] H. V. Peiris *et al.*, Astrophys. J., Suppl. Ser. **148**, 213 (2003).
[2] Supernova Search Team Collaboration, A. G. Riess *et al.*, Astron. J. **116**, 1009 (1998).
[3] Supernova Cosmology Project Collaboration, S. Perlmutter *et al.*, Astrophys. J. **517**, 565 (1999).
[4] E. Mottola, Phys. Rev. D **31**, 754 (1985).
[5] B. Allen, Phys. Rev. D **32**, 3136 (1985).
[6] T. S. Bunch and P. C. Davies, Proc. R. Soc. London **A360**, 117 (1978).
[7] N. D. Birrell and P. C. W. Davies, *Quantum Fields in Curved Space* (Cambridge University Press, Cambridge, England, 1989).
[8] R. Floreanini, C. T. Hill, and R. Jackiw, Ann. Phys. (N.Y.) **175**, 345 (1987).
[9] N. Kaloper, M. Kleban, A. Lawrence, S. Shenker, and L. Susskind, J. High Energy Phys. **11**, 037 (2002).
[10] J. S. Schwinger, J. Math. Phys. **2**, 407 (1961).
[11] L. V. Keldysh, Zh. Éksp. Teor. Fiz. **47**, 1515 (1964) [Sov. Phys. JETP **20**, 1018 (1965)].
[12] U. H. Danielsson, Phys. Rev. D **66**, 023511 (2002); J. High Energy Phys. **12**, 025 (2002).
[13] A. Kempf, Phys. Rev. D **63**, 083514 (2001); A. Kempf and J. C. Niemeyer, *ibid.* **64**, 103501 (2001).
[14] R. Easther, B. R. Greene, W. H. Kinney, and G. Shiu, Phys. Rev. D **64**, 103502 (2001); **67**, 063508 (2003).
[15] S. Shankaranarayanan, Class. Quantum Grav. **20**, 75 (2003).
[16] R. Easther, B. R. Greene, W. H. Kinney, and G. Shiu, Phys. Rev. D **66**, 023518 (2002).
[17] K. Goldstein and D. A. Lowe, Phys. Rev. D **67**, 063502 (2003).
[18] J. Martin and R. Brandenberger, Phys. Rev. D **68**, 063513 (2003).
[19] H. Collins and M. Martin, hep-ph/0309265.
[20] T. Banks and L. Mannelli, Phys. Rev. D **67**, 065009 (2003).
[21] M. B. Einhorn and F. Larsen, Phys. Rev. D **67**, 024001 (2003).
[22] M. B. Einhorn and F. Larsen, Phys. Rev. D **68**, 064002 (2003).
[23] K. Goldstein and D. A. Lowe, Nucl. Phys. **B669**, 325 (2003).
[24] R. Bousso, A. Maloney, and A. Strominger, Phys. Rev. D **65**, 104039 (2002).
[25] For an excellent review of de Sitter space, its causal structure and its coordinatizations, see M. Spradlin, A. Strominger, and A. Volovich, hep-th/0110007.
[26] K. T. Mahanthappa, Phys. Rev. **126**, 329 (1962); P. M. Bakshi and K. T. Mahanthappa, J. Math. Phys. **4**, 12 (1963).
[27] D. Boyanovsky, H. J. de Vega, and S. Y. Wang, Phys. Rev. D **61**, 065006 (2000).